

# **Cyclodextrin-mediated crystallization of acid $\beta$ -glucosidase in complex with amphiphilic bicyclic nojirimycin analogues**

**Boris Brumshtein, Matilde Aguilar-Moncayo, Juan M. Benito, José M. García  
Fernandez, Israel Silman, Yoseph Shaaltiel, David Aviezer, Joel L. Sussman, Anthony H.  
Futerman and Carmen Ortiz Mellet**

## **Supporting Information**

### **List of Contents:**

- .- S1            General procedure for the inhibition assay.**
- .- S1            Tensiometry.**
- .- S2 to S6     Figures S1 and S4 showing Lineweaver-Burk plots for  $K_i$   
determinations.**
- .- S7 and S8   Figures S5 to S9 showing titration plots for NOI-NJ and 6-S-  
NOI-NJ with  $\beta$ -cyclodextrin.**
- .- S8 to S11   Figures S10 to S13 showing the NMR spectra of compounds  
NOI-NJ and 6-S-NOI-NJ in the absence and in the presence of  
 $\beta$ -cyclodextrin.**

**General procedure for the inhibition assay against recombinant  $\beta$ -glucocerebrosidase (prGCD).** Inhibition constant ( $K_i$ ) values were determined by spectrophotometrically measuring the residual hydrolytic activities of prGCD against *p*-nitrophenyl  $\beta$ -D-glucopyranoside in the presence of NOI-NJ or 6S-NOI-NJ. Each assay was performed in phosphate buffer (pH 7.3) or phosphate-citrate buffer (pH 5.5). The reactions were initiated by addition of enzyme to a solution of the substrate in the absence or presence of various concentrations of inhibitor. The mixture was incubated for 10-30 min at 37 °C and the reaction was quenched by addition of 1 M  $\text{Na}_2\text{CO}_3$ . Reaction times were appropriate to obtain 10-20% conversion of the substrate in order to achieve linear rates. The absorbance of the resulting mixture was determined at 405 nm. Approximate values of  $K_i$  were determined using a fixed concentration of substrate (around the  $K_M$  value for the different glycosidases) and various concentrations of inhibitor. Full  $K_i$  determinations and enzyme inhibition mode were determined from the slope of Lineweaver-Burk plots and double reciprocal analysis. Representative examples of the Lineweaver-Burk plots, with typical profile for competitive inhibition mode, are shown in Figures S1 to S4.

**Tensiometry.** The surface tension of NOI-NJ and 6S-NOI-NJ was measured in phosphate-citrate buffer (pH 5.5) and phosphate buffer (pH 7.3) with a homemade tensiometer based on a Mettler Toledo AL 204 balance.

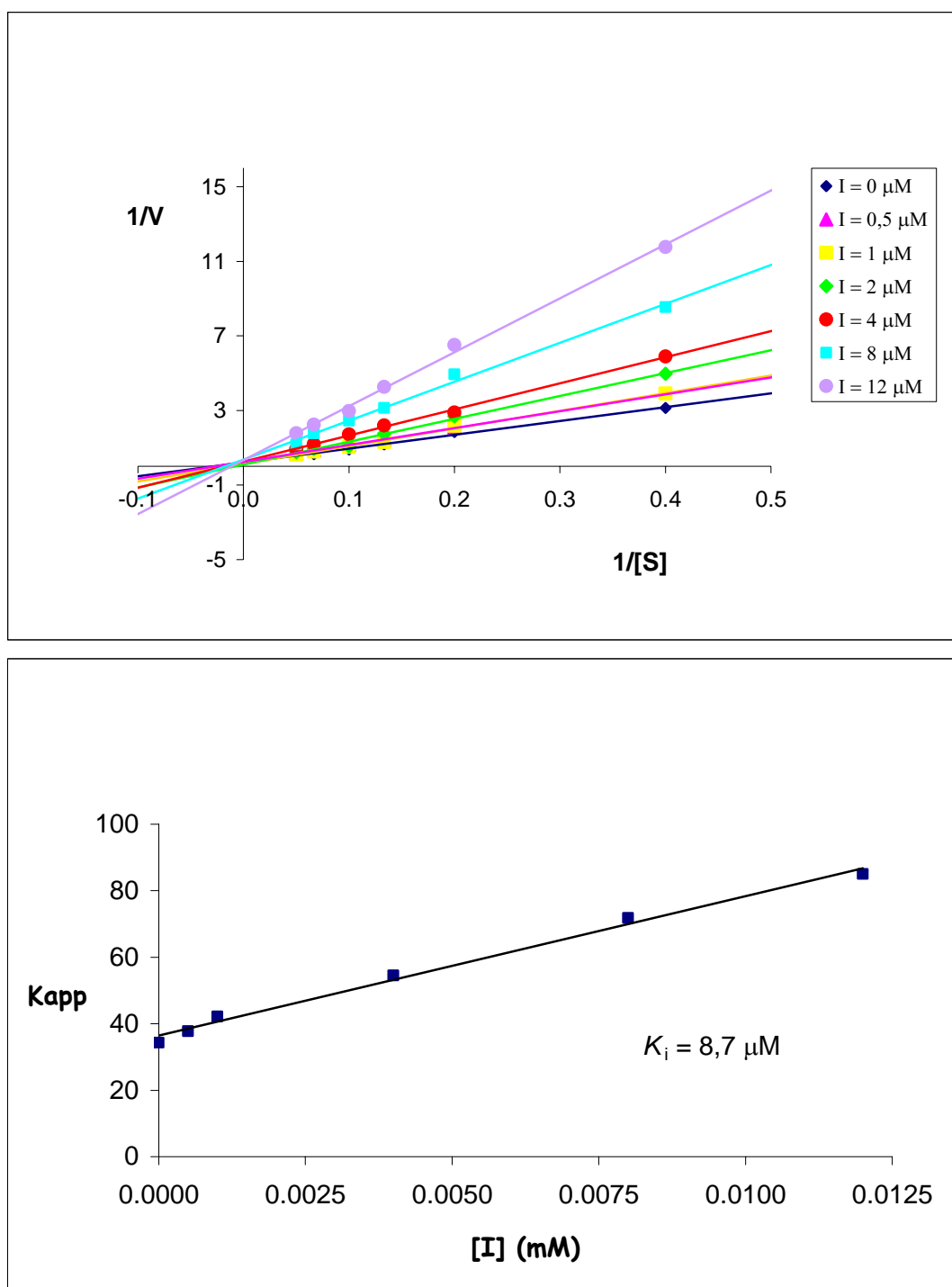


**Figure S1.** Lineweaver-Burk Plot for  $K_i$  determination (8.7  $\mu\text{M}$ ) of NOI-NJ against prGCD (pH 5.5).

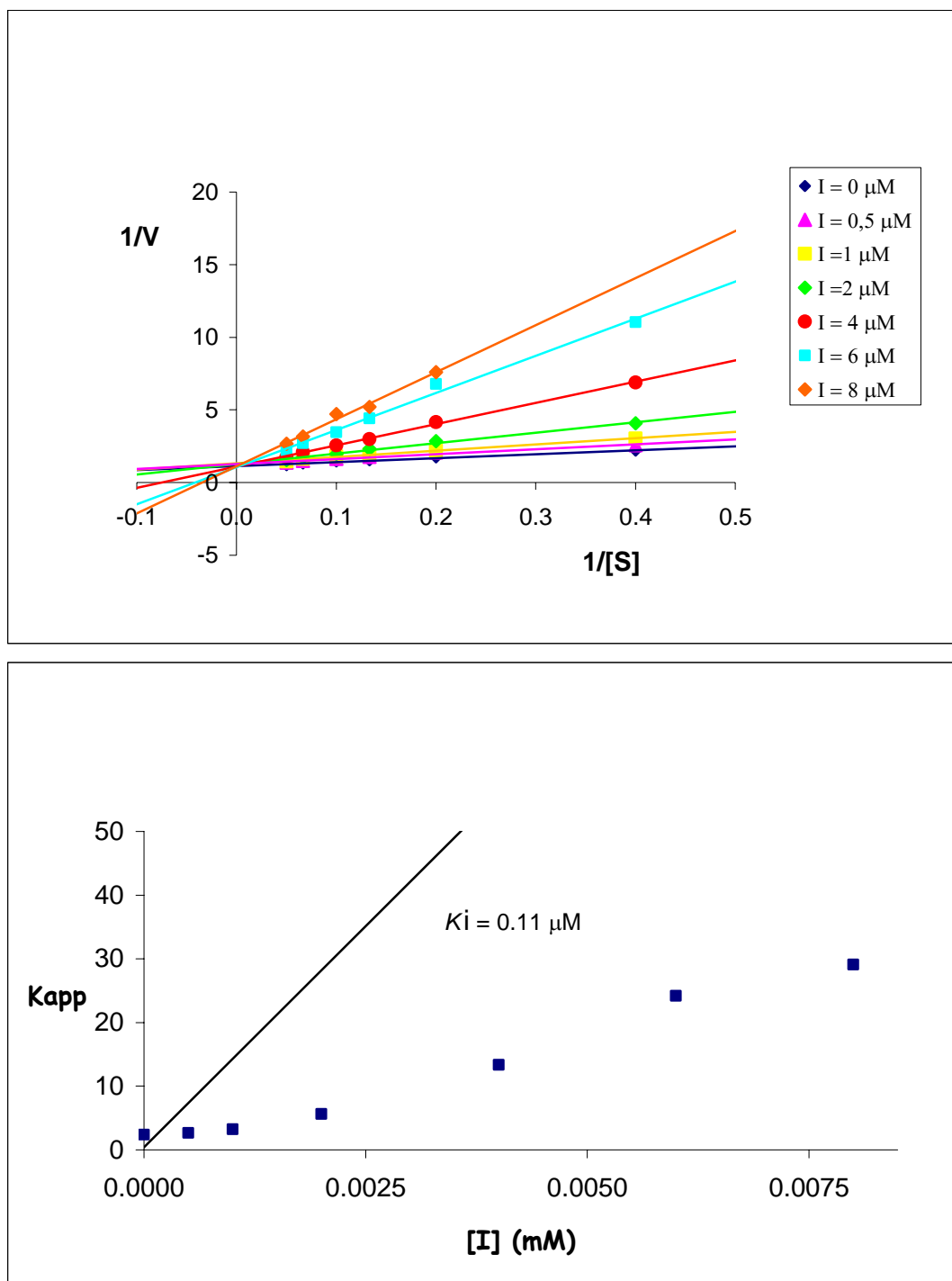


**Figure S2.** Lineweaver-Burk Plot for  $K_i$  determination ( $0.11 \mu\text{M}$ ) of NOI-NJ against prGCD (pH 7.3).

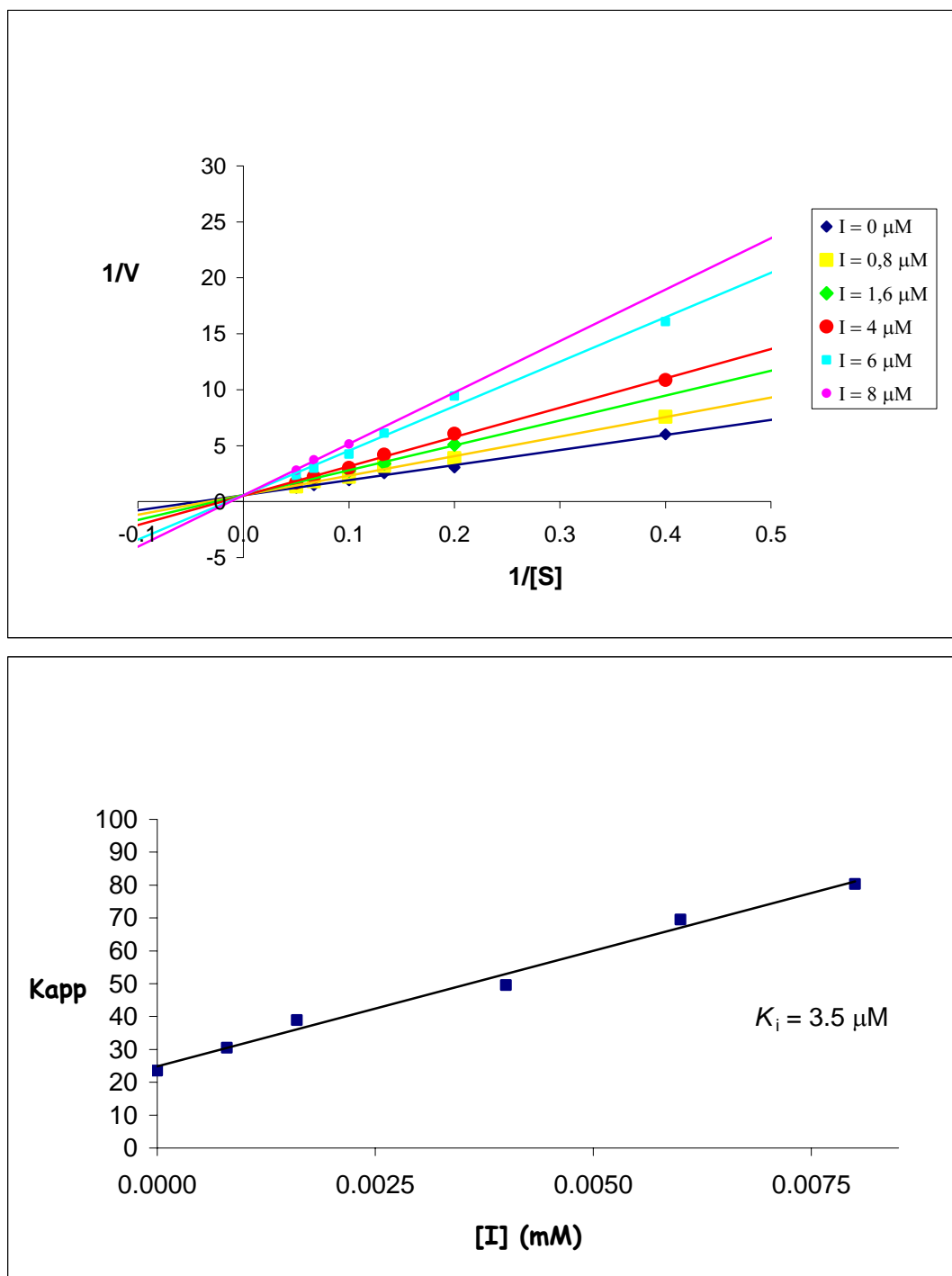


**Figure S3.** Lineweaver-Burk Plot for  $K_i$  determination ( $3.5 \mu\text{M}$ ) of 6-S-NOI-NJ against prGCD (pH 5.5).

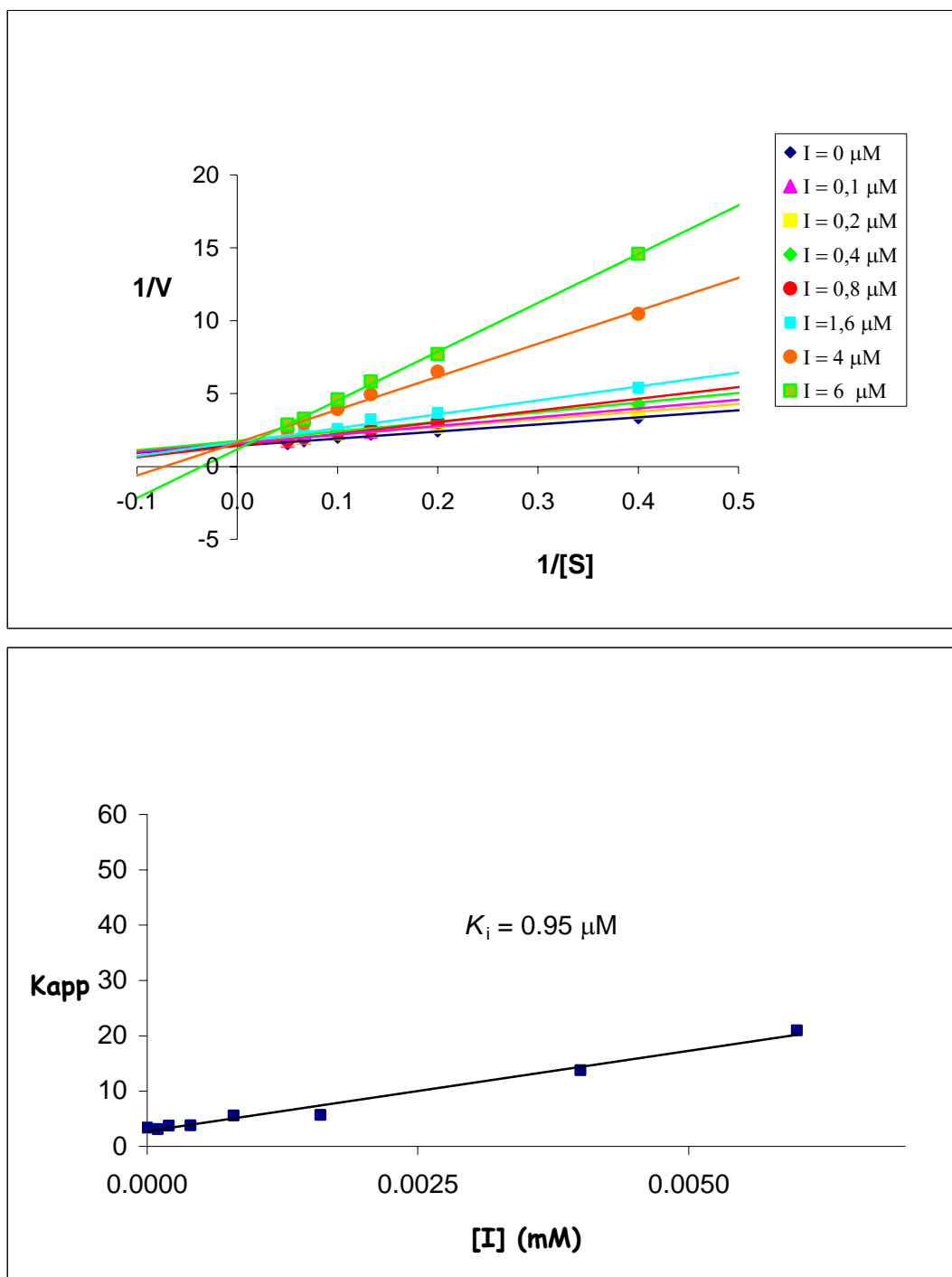


**Figure S4.** Lineweaver-Burk Plot for  $K_i$  determination ( $0.95 \mu\text{M}$ ) of 6-S-NOI-NJ against prGCD (pH 7.3).

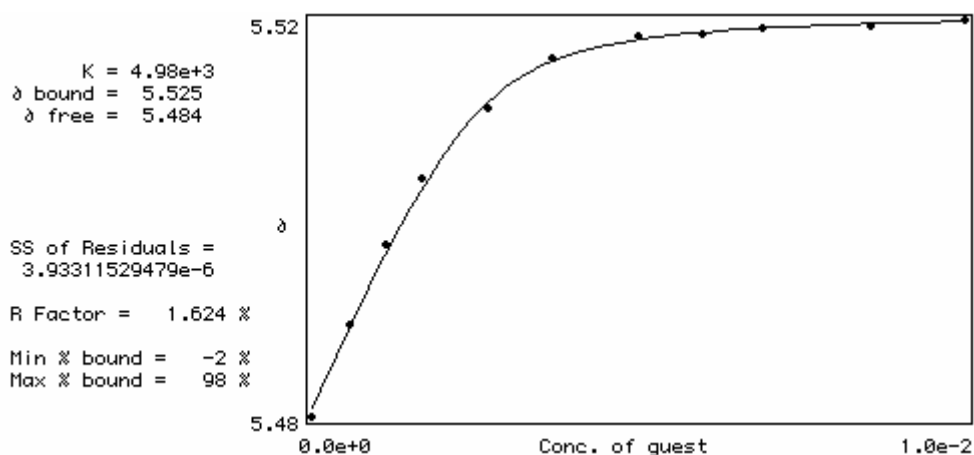


**Figure S5.** Titration plot obtained from the changes in the chemical shift of the H-1 resonance of NOI-NJ (2.64 mM) in the presence of increasing concentrations of  $\beta$ CD.

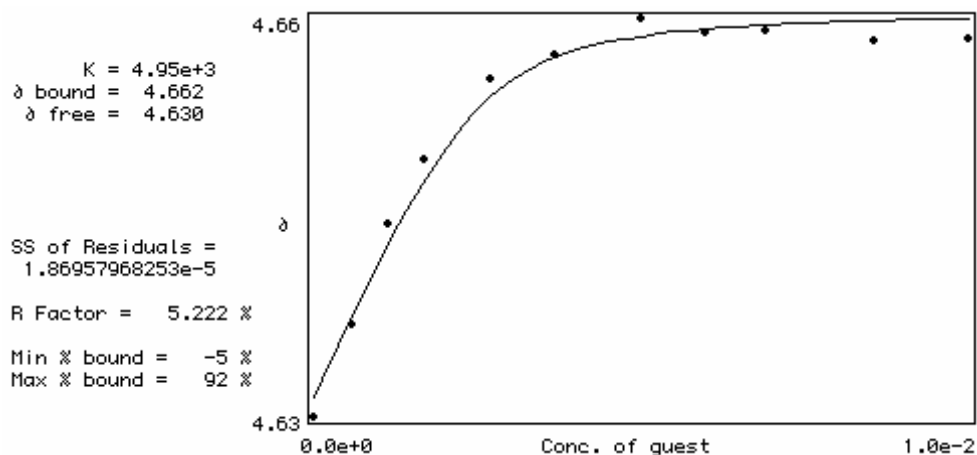


**Figure S6.** Titration plot obtained from the changes in the chemical shift of the H-6a resonance of NOI-NJ (2.64 mM) in the presence of increasing concentrations of  $\beta$ CD.

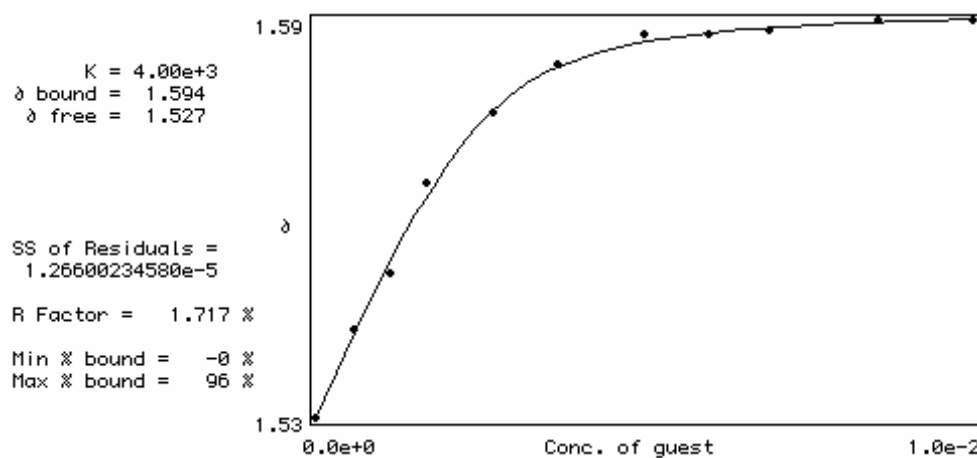


**Figure S7.** Titration plot obtained from the changes in the chemical shift of the H-6a resonance of NOI-NJ (2.64 mM) in the presence of increasing concentrations of  $\beta$ CD.

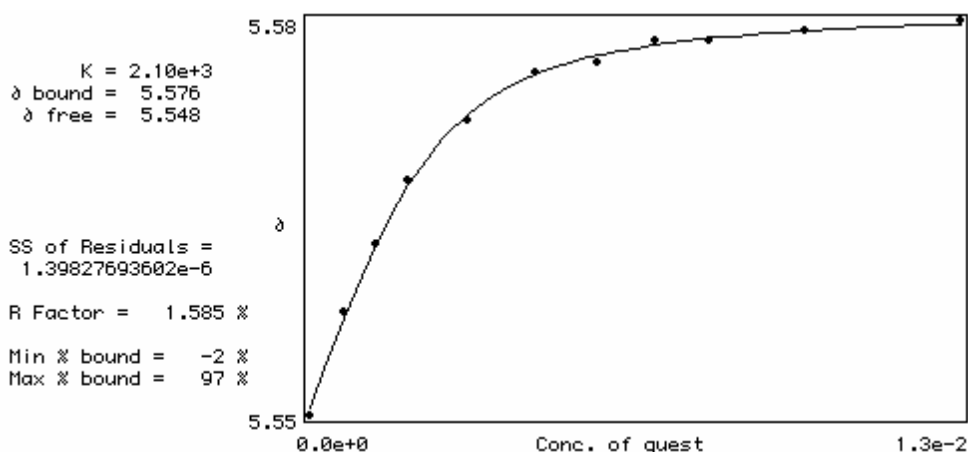


**Figure S8.** Titration plot obtained from the changes in the chemical shift of the H-1 resonance of 6S-NOI-NJ (2.41 mM) in the presence of increasing concentrations of  $\beta$ CD

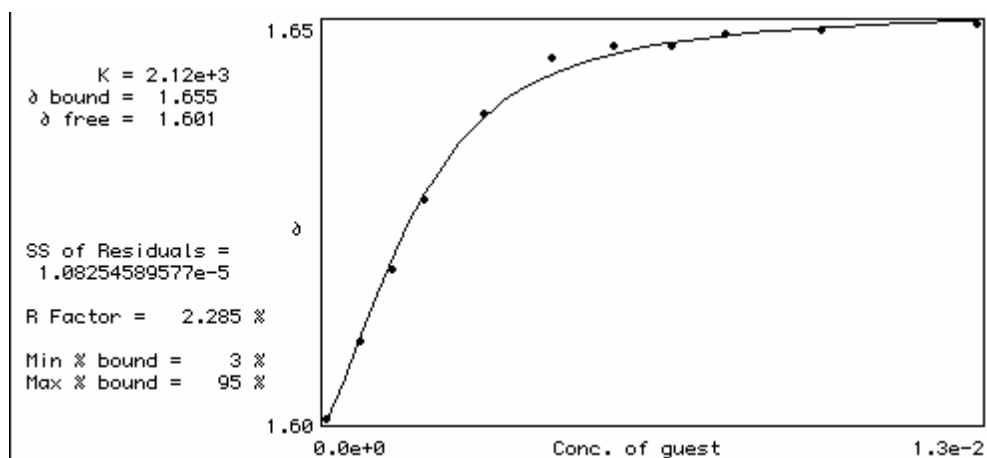


**Figure S9.** Titration plot obtained from the changes in the chemical shift of the H-6a resonance of 6S-NOI-NJ (2.41 mM) in the presence of increasing concentrations of  $\beta$ CD.

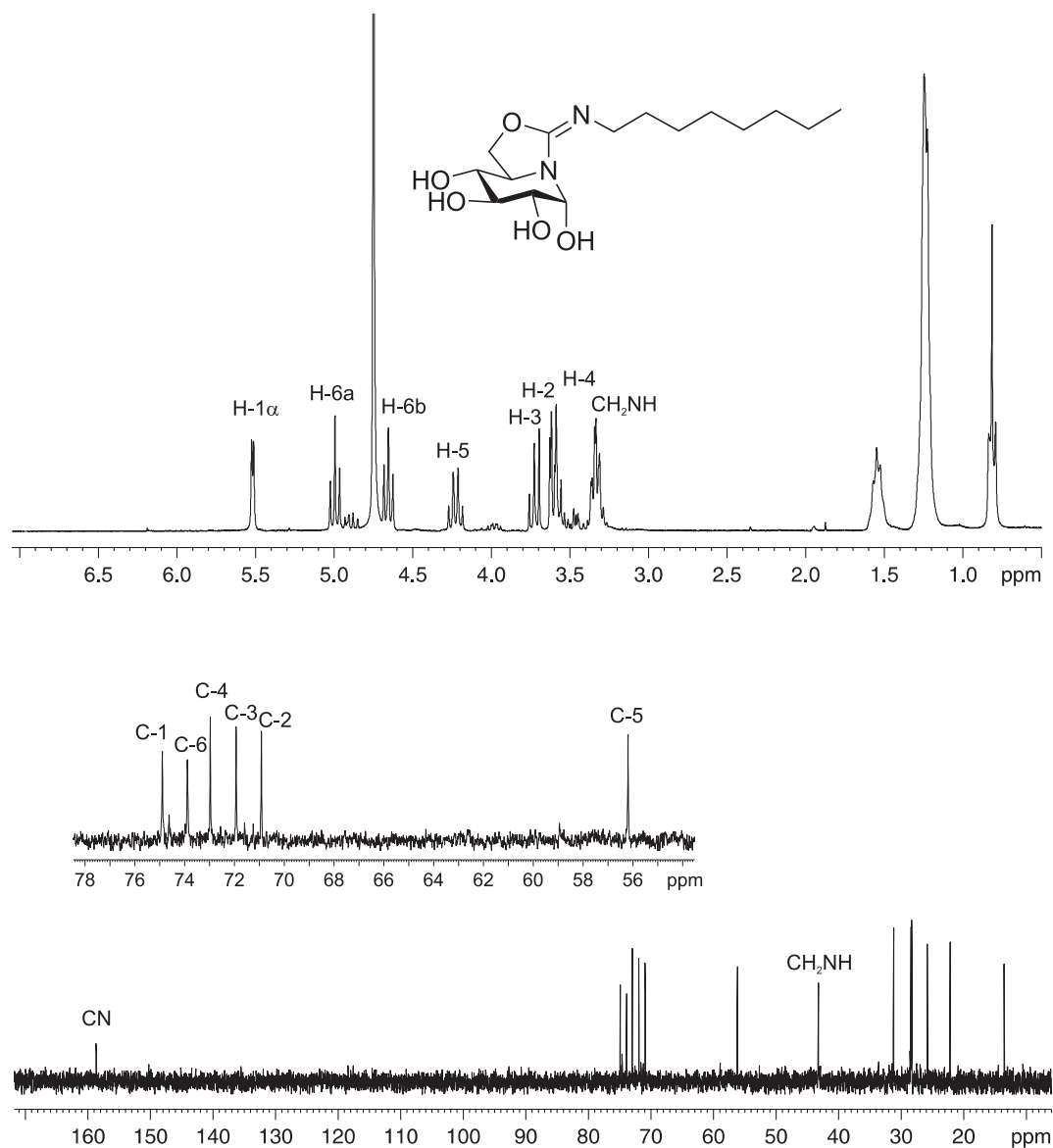


**Figure S10.**  $^1\text{H}$  and  $^{13}\text{C}$  NMR spectra (300 MHz, 75.5 MHz,  $\text{D}_2\text{O}$ ) of NOI-NJ.

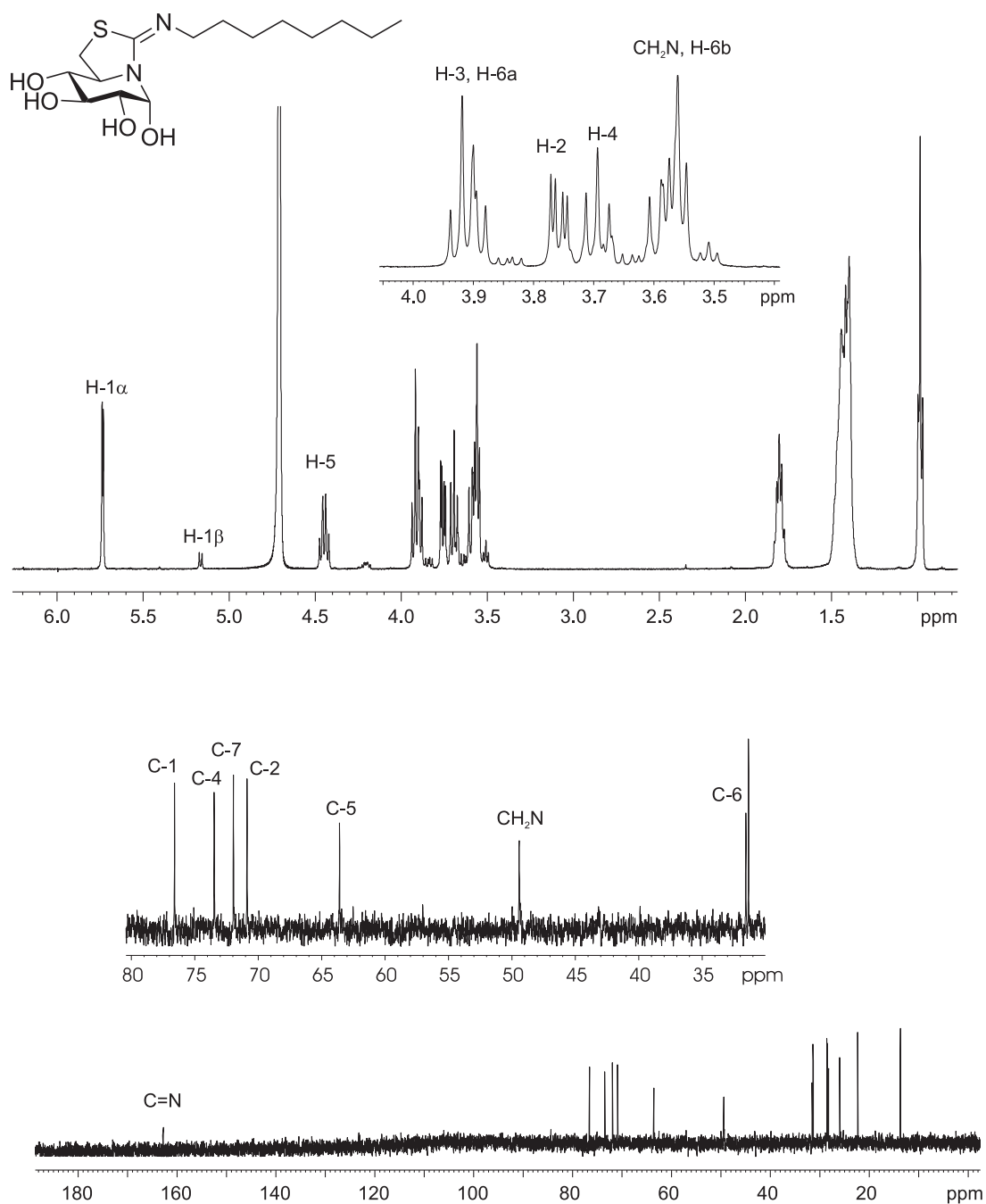


**Figure S11.**  $^1\text{H}$  and  $^{13}\text{C}$  NMR spectra (500 MHz, 75.5 MHz,  $\text{D}_2\text{O}$ ) of 6S-NOI-NJ.

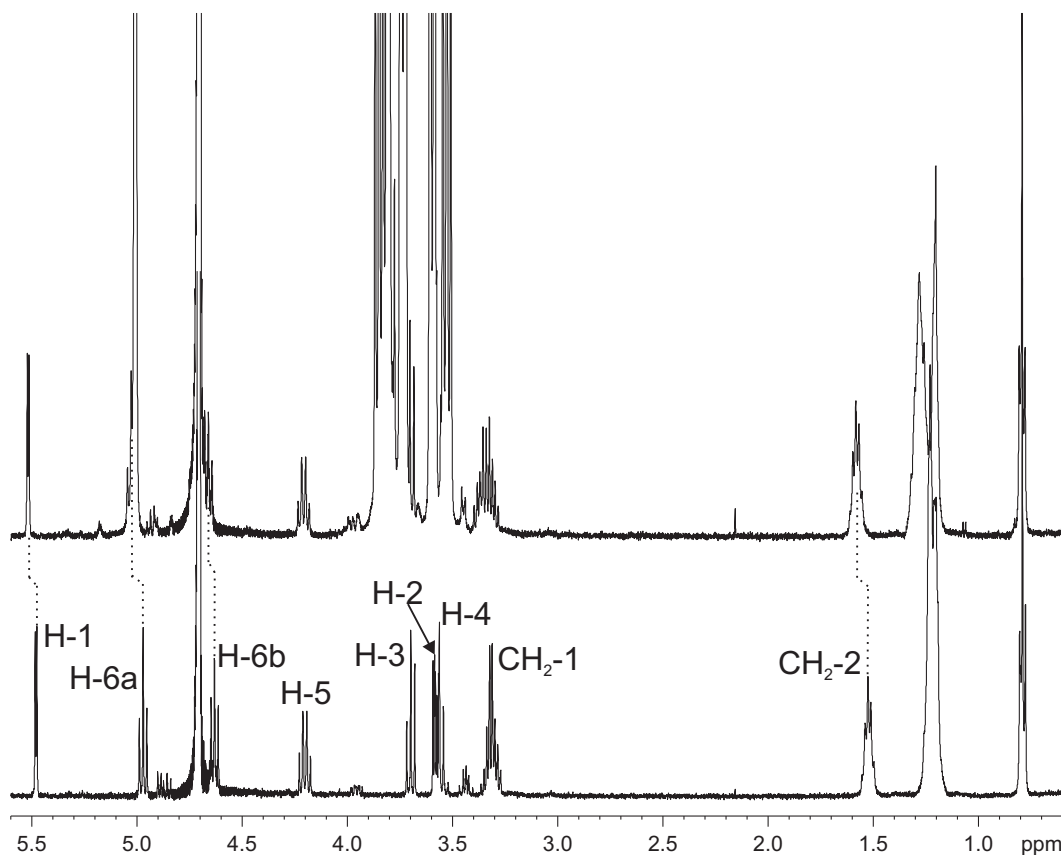


**Figure S12.** Comparative  $^1\text{H}$  NMR Spectra of NOI-NJ (2.64 mM, 500 MHz, 298 K,  $\text{D}_2\text{O}$ ) in the absence (bottom) and in the presence of  $\beta\text{CD}$  (1:1.4 NOI-NJ: $\beta\text{CD}$  ratio; top).

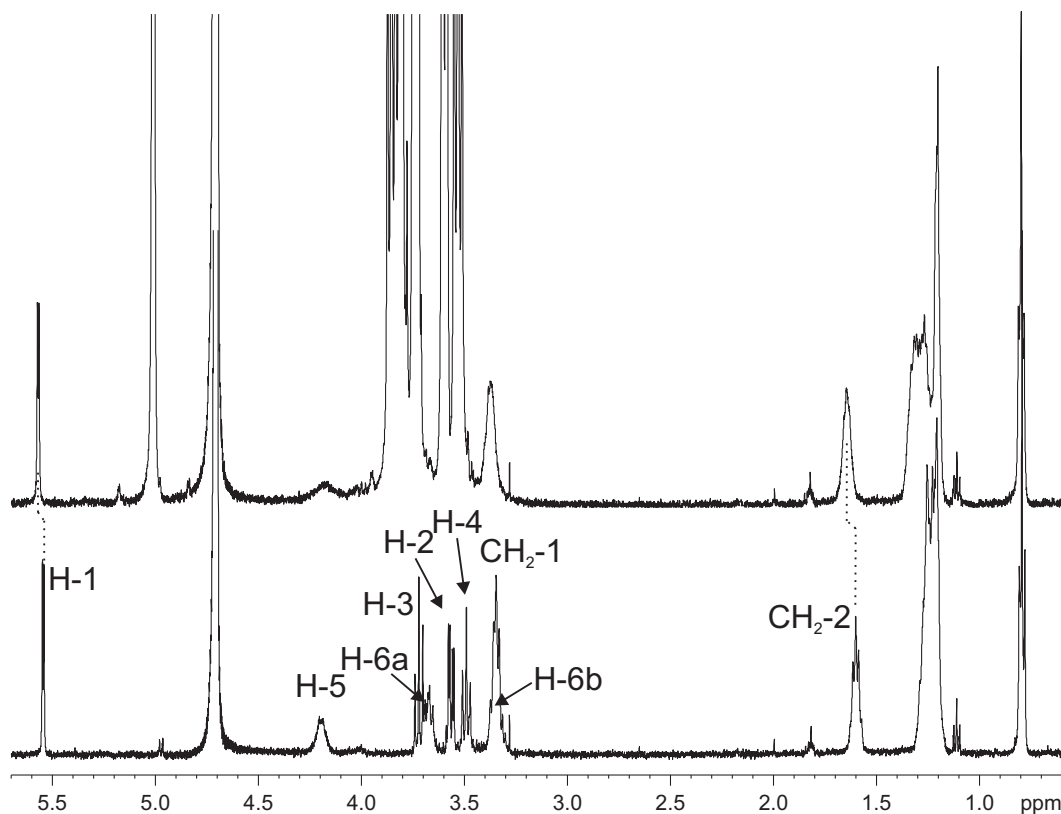


**Figure S13.** Comparative  $^1\text{H}$  NMR Spectra of 6S-NOI-NJ (2.41 mM, 500 MHz, 298 K,  $\text{D}_2\text{O}$ ) in the absence (bottom) and in the presence of  $\beta\text{CD}$  (1:1.7 6S-NOI-NJ: $\beta\text{CD}$  ratio; top).